Journal of Integrative Neuroscience

J. Integr. Neurosci. **2022**; 21(5): 147
https://doi.org/10.31083/j.jin2105147

Original Research

Proteomic Analysis of the Sphincter in a Neurogenic Bladder Caused by T10 Spinal Cord Injury

Qi-Rui Qu[1], Li-Ya Tang[1], Qiong Liu[1], Yi-Ying Long[1], Xia Wu[1], Ming Xu[1], Fang Qi[1], Hong Zhang[1], Kun Ai[1,*], Lu Zhou[2,*]

[1]College of Acupuncture, Massage and Rehabilitation, Hunan University of Chinese Medcine, 410208 Changsha, Hunan, China
[2]Department of Rehabilitation Medicine, Chenzhou First People's Hospital, 423000 Chenzhou, Hunan, China
*Correspondence: ak_kunai@outlook.com (Kun Ai); Zhoulu0316@outlook.com (Lu Zhou)
Academic Editor: Rafael Franco
Submitted: 18 February 2022 Revised: 12 May 2022 Accepted: 22 June 2022 Published: 26 August 2022

Abstract

Objective: This study aimed to conduct proteomic analysis of the sphincter in a neurogenic bladder caused by T10 spinal cord injury. The differentially expressed proteins (DEPs) of the sphincters (internal urethral sphincter) in the neurogenic bladders (NBs) of rats after complete transection of the T10 spinal cord segment were screened using tandem mass tag (TMT)-based quantitative labeling, and their biological information was analyzed. **Methods**: Twelve adult Sprague Dawley rats out of 40 were randomly assigned to the blank group ($n = 12$), while the remaining 28 were placed in the T10 spinal cord injury model via modified Hassan Shaker spinal cord transection; 12 of these rats were then randomly selected as the model group. The rats in both groups underwent urodynamics detection and hematoxylin and eosin (H&E) staining. The proteins expressed in the bladder sphincter were detected using TMT-based quantitative proteomics. DEPs were defined as proteins with fold change >1.5 or $<1/1.5$, $p < 0.05$, and unique peptide ≥ 2. The DEPs were subjected to Kyoto Encyclopedia of Genes and Genomes (KEGG) pathway enrichment analysis using KOBAS 3.0., and gene ontology functional annotation analysis was performed using the Cytoscape 3.7.1. BiNGO plug-in. The protein–protein interaction network was then constructed using the interactive gene-retrieval tool STRING and Cytoscape software. **Results**: The leak-point pressure and maximum cystometric volume in the model group were significantly higher than those in the blank group ($p < 0.01$), and H&E staining showed continuous interruption of the bladder sphincter fibers in the model group. A total of 250 DEPs were screened in the bladder sphincter, 83 of which were up-regulated and 167 of which were down-regulated. KEGG analysis of the DEPs was used to screen 15 pathways, including metabolic pathways, extracellular matrix (ECM)-receptor interaction, adhesion spots, the phosphoinositide 3-kinase (PI3K)/protein kinase B (Akt) signaling pathway, the cytochalasin signaling pathway, and the advanced glycation end-products (AGE)/receptor for AGEs (RAGE) signaling pathway in diabetic complications and vascular smooth muscle contraction. **Conclusions**: It is of great significance to explore the pathological mechanism of non-inhibitory contraction of the bladder sphincter caused by spinal cord injury above the T10 segment from the perspective of ECM-receptor interaction, focal adhesion-activated PI3K/Akt signaling pathway, and cell relaxation signaling pathways. Synaptic vesicle glycoprotein (Sv2A) involved in the release of neurotransmitters from synaptic vesicles, arrestin $\beta 2$ inhibitory proteins involved in α-adrenergic receptors and G-protein-coupled receptor internalization, and calmodulin and calmodulin binding protein involved in calcium-sensitive signaling pathways may be potential targets for developing new ways to treat bladder sphincter overactivity caused by T10 spinal cord injury.

Keywords: suprasacral spinal cord injury; neurogenic bladder; bladder sphincter (internal urethral sphincter); proteomics; differentially expressed proteins; bioinformatics analysis

1. Introduction

A neurogenic bladder (NB) is a common complication of spinal cord injury [1]. Bladder dysfunction caused by complete injury of the T10 and above spinal cord segment is often characterized by simultaneous non-inhibitory contraction of the detrusor, bladder sphincter (internal urethral sphincter) and/or external urethral sphincter, resulting in increased internal bladder pressure [2], it manifests as urine retention, which may cause renal reflux and, over time, renal damage, eventually leading to renal failure in severe cases [3].

Previous research has revealed that the bladder sphincter, external urethral sphincter, and urethral mucosa each account for a third of micturition control [4].

The bladder sphincter is located at the bladder neck and is doubly innervated by sympathetic (T11-L2) and parasympathetic (S2-S4) nerves, which have the function of controlling urination. Under normal conditions, parasympathetic excitation of the bladder during urination and inhibition of the sympathetic nerves cause contraction of the detrusor muscle and diastole of the bladder sphincter, producing urination. After an injury above the mid-thoracic spinal cord, the sympathetic and parasympathetic regions of the spinal cord, which innervate the bladder sphincter, lose control of the higher centers and become synergistically impaired, with continued sympathetic excitation and

increased release of norepinephrine in the bladder sphincter, causing continuous contraction of the bladder sphincter, resulting in increased pressure at the urethral outlet during urination and impaired urination [5,6]. Therefore, the idea of clinical treatment for neurogenic bladder with synergistic dysfunction of the detrusor-vesical sphincter (bladder neck) should be to suppress overactivity of the bladder sphincter. Current studies have focused on the bladder forced urinary muscle and the external urethral sphincter, and relatively little research has been done on the bladder sphincter. Clinical treatment of bladder neck dysfunction by cystotomy [7] and α-blockers [8] has also been reported, and although some efficacy has been achieved, there are still drawbacks such as postoperative complications and drug side effects. Therefore, the search for other potential targets of intervention to guide the treatment of bladder neck dysfunction after spinal cord injury is particularly important in clinical aspects.

Bioinformatics analysis focuses on exploring potential therapeutic targets; it can evaluate the pathological mechanism of a disease from multiple angles [9]. Tandem mass tag (TMT)-based quantitative labeling technology can comprehensively detect the proteins expressed in tissues, and this technology also has high sensitivity and high-depth proteome coverage for the application of proteomics [10].

In the present study, a T10 spinal cord injury model was prepared by modifying the Hassan Shaker spinal cord transection method [11]. Differentially expressed proteins (DEPs) in the bladder sphincter were then detected using TMT-based quantitative labeling, and bioinformatics analysis was conducted on these DEPs to identify new biomarkers and targets to guide the treatment of NB.

2. Materials and Methods

2.1 Grouping of Experimental Animals

A total of 40 healthy adult female specific pathogen-free rats, weighing 250–280 g, were obtained from the Animal Center Laboratory of Hunan University of Traditional Chinese Medicine (certificate no.: 1107271911006889). The rats were given one week of adaptive feeding under standard conditions (temperature 24–26 °C, humidity 50–70%) in cages in the Animal Center Laboratory of Hunan University of Traditional Chinese Medicine. They were then randomly divided into two groups: a blank group (n = 12) and a model group (n = 28). The rats in the model group underwent T10 spinal cord injury via Hassan Shaker spinal cord transection, with a total of 25 surviving after spinal cord shock, 13 of which developed urinary retention. A total of 12 of the rats were selected by random number table and included in the final model group.

2.2 Main Reagents and Instruments

Cell and tissue total protein extraction kit (Kangchen Bio-tech, Shanghai, China); KC™ chemiluminescence kit (Kangchen Bio-tech, Shanghai, China); bicinchoninic acid (BCA) protein quantitative kit (Kangchen Bio-tech, Shanghai, China); 3% pentobarbital sodium (Merck KGaA, San Jose, CA, USA); penicillin sodium (North China Pharmaceutical, Shijiazhuang, Hebei, China); MP150-WSW multichannel physiological signal recorder (Biopac, Goleta, CA, USA); WZ-50C6 dual-channel micro injection pump (factory No.: 150202698, Smiths Medical Instrument, Jiaxing, Zhejiang, China); automatic biochemical analyzer (Toshiba, Tokyo, Japan).

2.3 Modeling

Two hours before modeling, 200,000 units of penicillin sodium were injected intraperitoneally to prevent inflammation. Intraperitoneal anesthesia was then administered with 3% pentobarbital sodium (50 mg/kg). The rats were placed prone and fixed on a rat plate, with the 13th thoracic vertebra as the bone marker. Skin preparation and disinfection were undertaken at the 8th–9th thoracic vertebrae, after which a longitudinal incision of 2–3 cm was made and the subcutaneous tissue was cut. The bilateral erector spinalis and paraspinous muscles were bluntly separated to expose the spinous processes of T8 and T9 and the adjacent vertebral arch. The T8 lamina and bilateral pedicle were removed with a micro bone remover in order to expose the spinal cord. The spinal cord was then drawn out with a dental hook and transected with a no. 11 surgical blade; multiple transections were made to ensure complete severing of the spinal cord. The muscles were sutured, the incision and its surroundings were disinfected with 5% complex iodine, and the skin was sutured.

After the operation, the rats were placed on an electric blanket at a constant temperature until they regained consciousness, after which each rat was placed in a separate cage. Penicillin sodium (200,000 U/animal) was injected intraperitoneally in the morning and evening one week after the operation. Credé manipulation was used to assist urination in the morning, at noon, and in the evening every day. In the case of bedsores and self-mutilation, disinfection was undertaken with iodophor, and penicillin powder was sprinkled on the corresponding parts.

The rats in the blank group were routinely fed until the urodynamics test, and no other treatment was given during the period.

The rats in the T10 spinal injury model were assessed for hind-limb motor function and bladder-voiding function. For hind-limb motor function, the inability to move the hind limbs when walking, dragging on the front limbs, and the Basso, Beattie and Bresnahan (BBB) score [12] of 0 points were noted; for bladder-voiding function, urinary retention, bladder distention, and inability to autonomously urinate after the bladder shock period were noted. If these two conditions were met at the same time, the modeling was considered successful.

2.4 Observation Indexes and Detection Methods

Urodynamics was examined on the 18th day after modeling, after which the rats were euthanized through decapitation. The bladder sphincter was then removed and divided into two parts: one part was used for hematoxylin and eosin (H&E) staining, and the other was stored at –80 °C for TMT-based proteomics detection.

2.4.1 Urodynamics Test

On the 18th day after modeling, urodynamic examination was performed in the blank group and the model group. A bladder perfusion test was performed after anesthesia, during which an F3 catheter was inserted into the top of the bladder and placed horizontally with the bladder; the MP150 host pressure baseline was set to zero. The catheter, MP150-WSW 16-channel physiological recorder, and WZ-50C6 microinjection pump were connected through a three-way pipe. The microinjection pump was turned on and the perfusion rate was set to 6 mL/h at a temperature of 25–35 °C. Changes in the bladder pressure curve and urine leakage, including urine overflow from the urethral orifice, when urine overflow occurred for the first time, and leak-point pressure (LPP) at the time of first urine overflow, were then observed and recorded. The maximum cystometric capacity (MCC) was taken as the volume of fluid filled from the beginning of perfusion of normal saline to the leakage of urine from the urethral orifice. Perfusion continued until a stable waveform appeared.

2.4.2 H&E Staining

The right atrial appendage was cut after intraperitoneal injection of 3% pentobarbital sodium for anesthesia, and the left ventricle was rapidly perfused with normal saline until the outflow fluid became clear, after which the ventricle was fixed with 4% paraformaldehyde. The bladder neck was removed and fixed with 4% paraformaldehyde for 48 hours, after which it was rinsed, gradually dehydrated with ethanol, treated with xylene until it became transparent, soaked in wax, embedded, sliced into sections, stained, sealed with neutral gum, and observed under a light microscope.

2.5 TMT-Based Quantitative Analysis

2.5.1 Extraction of Protein Samples

The bladder sphincter was removed under 3% pentobarbital sodium anesthesia. Each sample was added to 1000 μL of working solution (a RIPA lysate was mixed with protease inhibitor and precooled on ice to obtain the working solution) and fully mixed, before being treated with ultrasound in an ice bath for five minutes until fully dissolved. It was then centrifuged at 14,000 $\times$ g at 4 °C for 15 minutes, after which the supernatant was transferred to a new Eppendorf tube. A BCA protein assay kit was used to quantitatively determine the protein concentration according to the manufacturer's instructions.

2.5.2 TMT Labeling

Each sample was subjected to high-speed centrifugation for 10 minutes, after which the supernatant was transferred to a new Eppendorf tube and the TMT was balanced to room temperature before opening. A total of 41 μL of anhydrous acetonitrile was added to the new Eppendorf, fully mixed and dissolved, and the TMT solution was collected by centrifugation. A total of 20 μL of TMT solution was then sucked into the corresponding sample, mixed well, and centrifuged, before being incubated at room temperature for one hour. Hydroxyl ammonia was added to the sample until the concentration reached 100 mM, and the reaction was terminated by incubation at room temperature for 15 minutes. The labeled samples of each group were mixed equally.

2.5.3 Liquid Chromatography-Tandem Mass Spectrometry (LC-MS/MS) Analysis

A total of 2 μg of polypeptide was taken from each component and separated using the nano-ultrahigh-pressure liquid chromatography liquid phase system EASY-NLC1200, before being analyzed using an online mass spectrometer (Q-Exactive). The analysis was conducted using 100 μm inside diameter (I.D.) $\times$ 15 cm reversed-phase chromatographic column (Reprosil-Pur 120 C18-AQ, 1.9 μm, Dr. Math). The sample was directly loaded into the chromatographic column by the automatic sampler then separated by chromatographic column. Flow rate was 300 nL/min, and the gradient duration was 90 minutes. Mobile phase B: 8–35% for 70 minutes, 35–45% for 12 minutes, 45–100% for 2 minutes, 100% for 2 minutes, 100–2% for 2 minutes, and 2% for 2 minutes.

2.5.4 MaxQuant Database Retrieval

The original data obtained after LC-MS/MS analysis were searched on MaxQuant (version 1.6.1.0, Thermo Scientific, Massachusetts, CA, USA) and subjected to TMT quantitative analysis; iBAQ non-standard quantification was performed at the same time. The false discovery rates of polypeptide and protein levels were <0.01. The samples were then standardized to ensure consistency in the total protein or median of each group.

DEPs were defined as proteins with fold change (FC) >1.5 or $<1/1.5$, $p < 0.05$, and unique peptide ≥ 2. Gene ontology (GO) functional annotation, Kyoto Encyclopedia of Genes and Genomes (KEGG) pathway enrichment, and protein–protein interaction (PPI) analysis were performed on all DEPs.

2.6 Bioinformatics Analysis of the Selected DEPs

The gene symbol corresponding to the DEPs was imported into KOBAS 3.0 [13] (http://kobas.cbi.pku.edu.cn/), and the species *Rattus norvegicus* was chosen to undergo KEGG pathway enrichment analysis, $p < 0.05$ for the Kyoto Encyclopedia of Genes and Genomes (KEGG) path-

way enrichment analysis. Genes and Genomes (KEGG) pathway enrichment analysis was performed, and the final enrichment results were sorted by input number; gene ontology (GO) functional annotation analysis was performed using the BiNGO plugin [14] in Cytoscape 3.7.1 (select species *Rattus. Norvegicus*, setting the parameter $p < 0.01$) and sorting the enrichment results by input number; PPI analysis of DEPs was performed using string 11.5 (https://cn.string-db.org/) and TSV format files were downloaded and imported into Cytoscape 3.7.1 software (National Institute of General Medical Sciences, Bethesda, MD, USA) [15] for further visualization; in addition, the MCODE (Molecular Complex Detection) plug-in was used to find key clusters and the Cluego plug-in was used to perform KEGG pathway enrichment analysis on these key clusters.

2.7 Statistical Analysis

Data were analyzed using statistical software SPSS 25.0 (International Business Machines Corporation, New York, NY, USA). Normally distributed measurement data were presented as mean ± standard deviation ($x \pm SD$), the means with homogeneity of variance were compared across groups using a *t*-test, and the means without homogeneity of variance were compared using the Wilcoxon test. Significant level was set as $\alpha = 0.05$.

3. Results

3.1 General Health

The general health of the rats in the blank group was good. In the rats in the model group, after the spinal cord shock period, the hind limbs were completely paralyzed, random movement disappeared, and the rats began dragging their hind limbs when walking. The rats also had urinary retention and bladder distension in the lower abdomen. The cages were slightly wet, and resistance at the urethral orifice could be felt during manual urination.

3.2 Urodynamics

The LPP and MCC in the model group were significantly higher than in the blank group ($p < 0.01$; see Table 1).

Table 1. Comparison of LPP and MCC of rats in each group (x ± SD).

Group	n	LPP (mmHg)	MCC (mL)
Blank group	12	19.362 ± 1.821	0.352 ± 0.188
Model group	12	39.643 ± 3.016*	4.740 ± 1.184*

Note: *, $p < 0.01$ compared with blank group.

3.3 H&E Staining

HE staining showed that the blanks group had a clear hierarchical structure of bladder sphincter tissue, with neat and tight arrangement of mucosal epithelium without detachment (①), and the lamina propria was full of elastic fibers without inflammatory cell infiltration; smooth muscle fibers were arranged in an orderly manner. Compared with the blank group, the mucosal epithelial layer of the bladder sphincter in the model group was thick, and the mucosal epithelium was detached in some areas (①); the intrinsic layer was infiltrated by a large number of inflammatory cells (②), and the elastic fibers were reduced; the nuclei of smooth muscle cells in the muscle layer were enlarged (③), and the muscle fibers were thickened and disordered, as shown in Fig. 1.

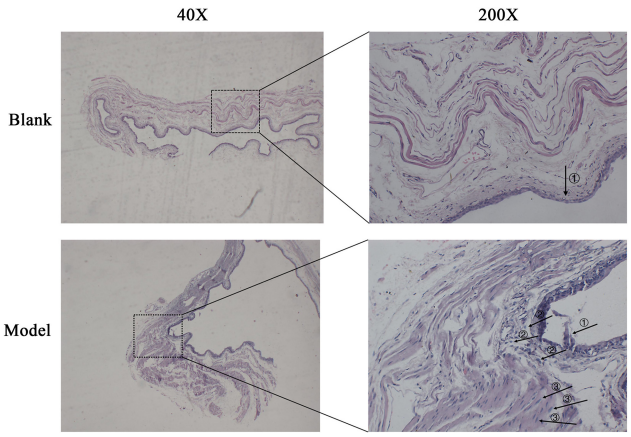

Fig. 1. Bladder sphincter injury by H&E staining. In the blank group, the tissue hierarchy of the bladder sphincter was clear, the mucosal epithelium was neatly and tightly arranged, and there was no shedding phenomenon (arrow ①). The lamina propria was full of elastic fibers without infiltration of inflammatory cells; smooth muscle fibers were arranged in an orderly manner. In the model group, the epithelial layer of the bladder sphincter mucosa was thicker, and the mucosal epithelium was sloughed off in some areas (arrow ①). A large number of inflammatory cells infiltrated in the lamina propria (arrow ②), and the elastic fibers decreased. The smooth muscle cell nucleus in the muscle layer is enlarged (arrow ③), the muscle fiber is hypertrophic, and the arrangement of the muscle fiber is disordered.

3.4 TMT-Based Analysis of DEPs

A total of 47,947 peptides and 6684 proteins were detected by TMT-based quantitative proteomics, 6099 of which were quantifiable proteins. According to the conditions of FC >1.5 or FC <1/1.5, $p < 0.05$, and unique peptide ≥2, 250 DEPs in the model group and blank group were screened, of which 83 were up-regulated and 167 were down-regulated (see Fig. 2).

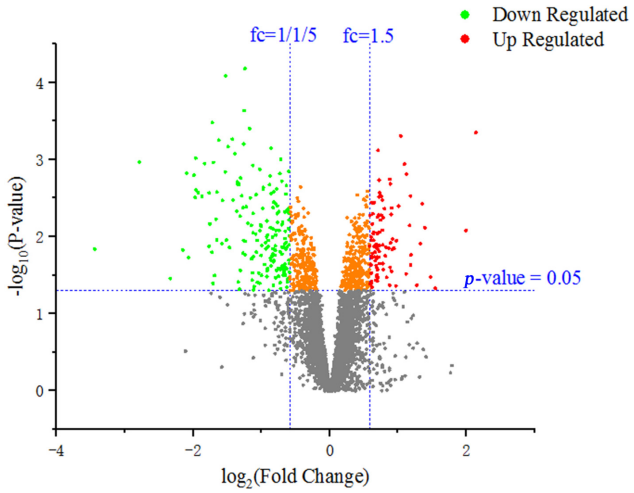

Fig. 2. Volcano diagram of 6099 proteins. Green represents down-regulated differentially expressed proteins (DEPs), red represents up-regulated DEPs, and gray represents proteins without differences of statistical significance.

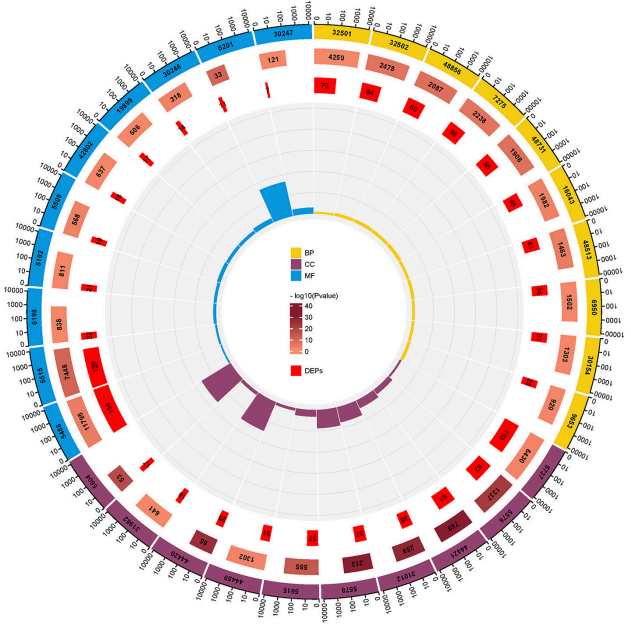

Fig. 3. GO functional annotation circle map of 250 DEPs. From outside to inside: GO classification annotation (yellow, purple and blue parts represent BP, CC and MF of 250 DEPs), the total number of proteins involved in this term in the database, the TMT quantitative proteome in this study The ratio of the number of DEPs screened out and involved in the term, the ratio of the number of DEPs involved in the term in the DEPs screened in this study to the total number of proteins involved in the term in the database.

3.5 Bioinformatic Analysis of DEPs

3.5.1 GO Functional Annotation Analysis of DEPs

GO functional annotation (including biological process [BP], cellular component [CC], and molecular function [MF]) was carried out using the Cytoscape BiNGO plug-in. With regard to BP, the DEPs were identified as being mainly involved in the cellular process, biological regulation, multicellular biological process, stress response, and negative regulation; with regard to CC, the DEPs were identified as being involved in the cytoplasmic region, extracellular region, plasma membrane, and vesicle of CC; and with regard to MF, the DEPs were identified as being involved in protein binding, structure, and molecular activity, receptor binding, calcium binding, enzyme site binding, and sugar binding proteins (see Fig. 3).

3.5.2 KEGG Pathway Analysis

KOBAS software was used for enrichment analysis of the KEGG pathways of the 250 identified DEPs, and a total of 15 KEGG pathways were selected with $p \leq 0.01$, including metabolic pathways, ECM-receptor interaction, adhesion spots, the phosphoinositide 3-kinase (PI3K)/protein kinase B (Akt) signaling pathway, cytochalasin signaling pathway, and the AGE-RAGE signaling pathway in diabetic complications and vascular smooth muscle contraction (see Fig. 4, Table 2).

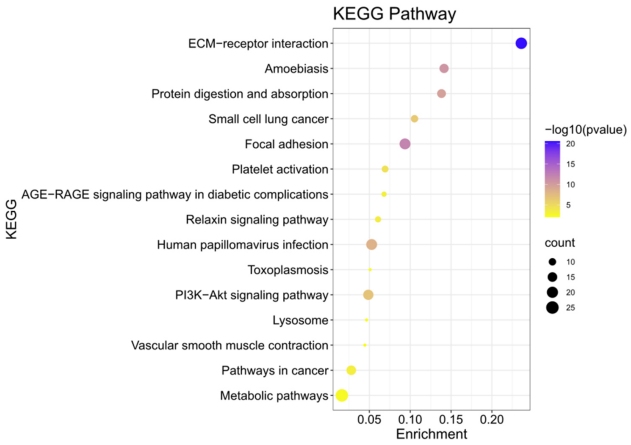

Fig. 4. Statistical bubble diagram of the Kyoto Encyclopedia of Genes and Genomes enrichment pathway. Enrichment is the ratio of the number of genes in the pathway to the total number of genes; the color and size of the dots represent the *p* value and the number of differentially expressed proteins in the pathway.

Table 2. KEGG pathway enrichment analysis of 250 DEPs.

Pathway	Input number	–log10 (Corrected *p*-value)	Input proteins
rno01100:Metabolic pathways	25	3.84	Gpi, H2afx, Oxct1, Cox7c, Glb1, Gpx3, Dpyd, Sms, Elovl1, Gstm4, Gclc, Pla2g2a, Ldha, Upp1, Spr, Nt5e, Akr1a1, Rpe, Abat, Naga, Glo1, Cox7a2, Pgk1, Hibch, Pafah1b2
rno04512:ECM-receptor interaction	21	23.40	Lama2, Col6a2, Lama4, Lama5, Fn1, Col6a1, Hspg2, Agrn, Lamb1, Col4a5, Lamc1, Col1a2, Col4a2, Col4a1, Col1a1, Sv2a, Vwf, Lamb2, Col6a5, Sv2c, Col6a6
rno04510:Focal adhesion	19	14.48	Lama2, Lamb2, Lama4, Lama5, Fn1, Col6a1, Col6a2, Lamb1, Col4a5, Lamc1, Col1a2, Col4a2, Col4a1, Col1a1, Myl12b, Vwf, Myl9, Col6a5, Col6a6
rno05165:Human papillomavirus infection	19	10.34	Lama2, Col6a2, Lama4, Lama5, Fn1, Stat2, Col6a1, Col4a5, Lamc1, Col1a2, Col4a2, Col4a1, Col1a1, Lamb1, Prkaca, Vwf, Lamb2, Col6a5, Col6a6
rno04151:PI3K-Akt signaling pathway	17	8.80	Lama2, Col6a2, Lama4, Lama5, Fn1, Col6a1, Col4a5, Lamc1, Col1a2, Col4a2, Col4a1, Col1a1, Lamb1, Vwf, Lamb2, Col6a5, Col6a6
rno05200:Pathways in cancer	15	4.89	Lama2, Lamc1, Lama4, Stat2, Fn1, Gstm4, Slc2a1, Col4a5, Prkaca, Col4a2, Col4a1, Lamb1, Calm2, Lamb2, Lama5
rno05146:Amoebiasis	14	13.03	Lama2, Lamc1, Lama4, Lama5, Fn1, Prkaca, Col4a5, Col1a2, Col4a2, Col4a1, Col1a1, Lamb1, Col3a1, Lamb2
rno04974:Protein digestion and absorption	13	12.02	Col15a1, Col7a1, Col14a1, Col4a5, Col1a2, Col4a2, Col4a1, Col1a1, Col6a1, Col3a1, Col6a2, Col6a5, Col6a6
rno05222:Small cell lung cancer	10	8.33	Lama2, Lamc1, Lama4, Lama5, Fn1, Col4a5, Col4a2, Col4a1, Lamb1, Lamb2
rno04611:Platelet activation	9	6.11	Myl12b, Col1a2, Col1a1, Prkaca, Col3a1, Vwf, Fgg, Fga, Fgb
rno04926:Relaxin signaling pathway	8	5.09	Arrb2, Col4a5, Col1a2, Col4a2, Col4a1, Col1a1, Prkaca, Col3a1
rno04933:AGE-RAGE signaling pathway in diabetic complications	7	4.82	Fn, Col4a5, Col1a2, Col4a2, Col4a1, Col1a1, Col3a1
rno05145:Toxoplasmosis	6	3.55	Lama2, Lamc1, Lama4, Lama5, Lamb1, Lamb2
rno04142:Lysosome	6	3.35	Lgmn, Ctsb, Glb1, Lamp1, Naga, Ap1g2
rno04270:Vascular smooth muscle contraction	6	3.25	Myl6, Calm2, Pla2g2a, Prkaca, Cald1, Myl9

3.5.3 Constructing the PPI of the Identified DEPs

To study the interaction between the 250 identified DEPs, the STRING online database and Cytoscape software were used to construct the PPI of the DEPs, with nodes representing the DEPs and lines representing interactions between proteins. Removing the DEPs without interactions, there were 229 nodes and 5374 edges in the PPI graph (Fig. 5). we screened out 7 clusters by using MCODE and performed KEGG pathway enrichment analysis on the 7 clusters using cluego. Cluster 1 was found to be mainly involved in signaling pathways such as ECM-receptor interaction, Focal adhesion, PI3K-Akt signaling pathway and Relaxin signaling pathway, while cluster 2 was involved in Amyotrophic lateral sclerosis (ALS) and Phototransduction pathway, cluster 3 is involved in Vascular smooth muscle contraction pathway, cluster 4 is mainly involved in Synthesis and degradation of ketone bodies and PPAR Cluster 4 is mainly involved in signaling pathways such as Synthesis and degradation of ketone bodies and PPAR signaling pathway, cluster 5 is mainly involved in signaling pathways such as Drug metabolism, cluster 6 is involved in signaling pathways such as Axon guidance, and cluster 7 is involved in Huntington disease pathway (Fig. 6).

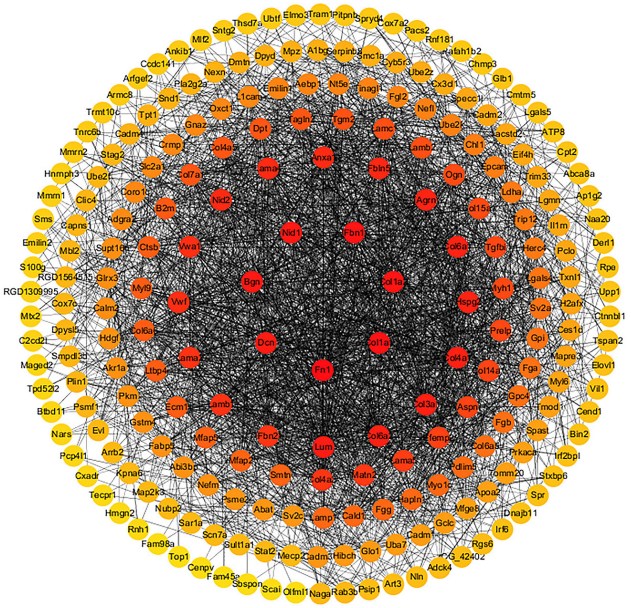

Fig. 5. The protein–protein interaction network of 244 differentially expressed proteins (DEPs); the red nodes indicate DEPs participating in Kyoto Encyclopedia of Genes and Genomes signaling pathways.

4. Discussion

After spinal cord injury above T10, the bladder sphincter, which is innervated by the T10-L2 sympathetic nerves, loses the control from the higher nerve center and has non-inhibitory contraction, resulting in bladder urination dysfunction [16]. The greatest clinical risk is the sudden increase in bladder pressure and large residual urine volume during voiding due to the inability of the bladder sphincter to relax at the same time as the contraction of the detrusor muscle, which can lead to recurrent urinary retention, urinary reflux, hydronephrosis and urinary tract infection, and even to renal failure. Because of the important role of the bladder sphincter in the voiding process, it is clinically useful to target it as a target site in the treatment of the detrusor-sphincter synergistic bladder disorder.

Therefore, we prepared a rat model of detrusor-sphincter synergistic dysfunctional bladder after transection injury of the T10 spinal cord segment, and the bladder sphincter (bladder neck) was selected as the object of observation in this study. The histomorphological results showed that, compared with the blank group, the mucosal epithelial layer of the bladder sphincter was thicker in the model group, with mucosal epithelial detachment in some areas; the lamina propria was heavily infiltrated with inflammatory cells and the elastic fibers were reduced; the smooth muscle cell nuclei in the muscle layer were enlarged, the muscle fibers were hypertrophied, and the muscle fibers were disorganized. In addition, urodynamics showed that both LPP and MCC were significantly higher in the bladder of the model group compared with the blank group, which suggested that the bladder sphincter and/or external urethral sphincter were excessively contracted after modeling, resulting in obstruction of urinary drainage, and thus LPP and MCC were significantly increased. Thus, a rat NB model of sphincter overactivity can be successfully caused by transection of the T10 spinal cord segment. We selected bladder sphincter (bladder neck) tissue and performed proteomic identification using TMT quantitative labeling technology to screen for differentially expressed proteins in bladder sphincter tissue, and the results showed that 250 DEPs were identified in the model/blank group of bladder sphincter. To explore potential clinical intervention targets for the disease, bioinformatic analysis was next performed on the differentially expressed proteins, and the results showed that these 250 DEPs were significantly enriched in 15 KEGG pathways. We focused on pathways closely related to the regulation of smooth muscle contraction, and the relevant DEPs were significantly enriched in extracellular matrix (ECM)-receptor interactions, adherent plaques, PI3K-Akt signaling pathway, cytosolic relaxin signaling pathway, and vascular smooth muscle contraction signaling pathway.

The three signaling pathways, extracellular matrix (ECM) receptor interactions, PI3K-Akt signaling pathway and adherent plaques, are very closely linked (Fig. 7A). Extracellular matrix (ECM) is a macromolecular material that is synthesized and secreted into the cell membrane or interstitial matrix, including collagen fibers, non-collagen fibers, elastic fibers, proteoglycans and aminoglycans. The complex network of ECMs not only has physical roles such as support, protection, and connectivity, but also exerts a

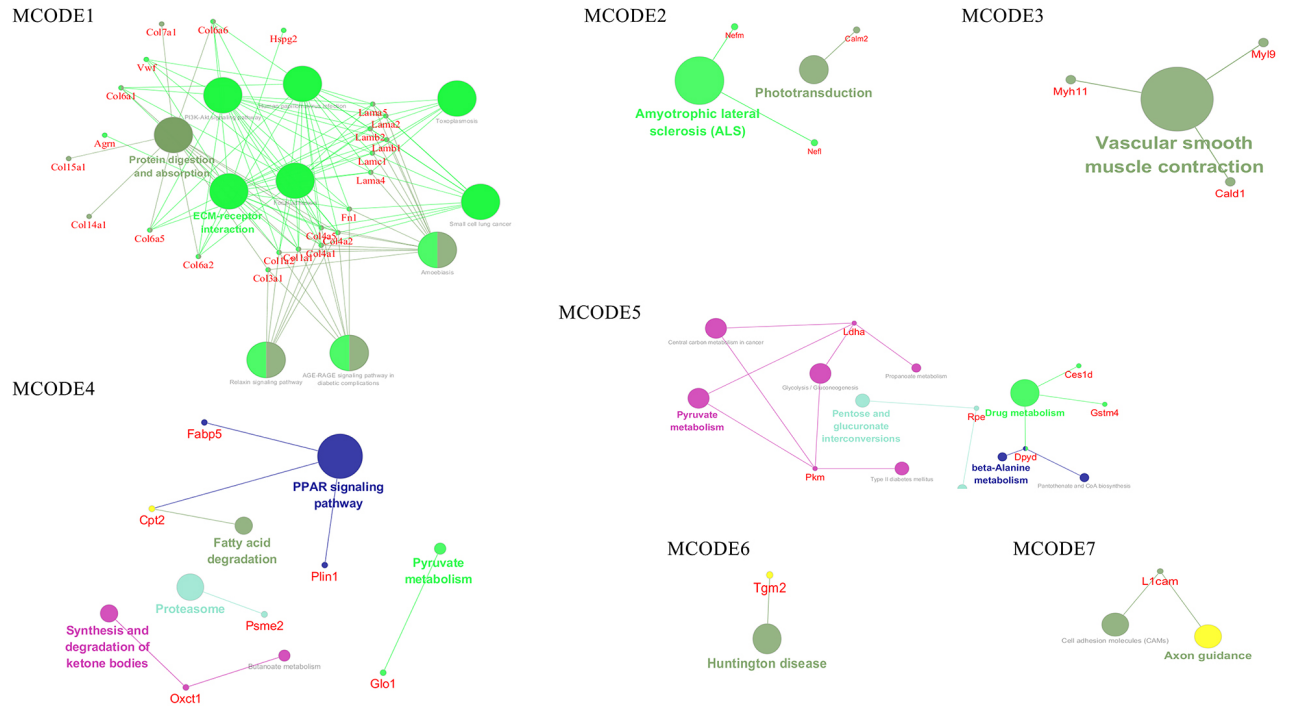

Fig. 6. ECM-receptor interaction, focal adhesion, phosphoinositide 3-kinase/protein kinase B signaling pathway, vascular smooth-muscle contraction and relaxin signaling pathway.

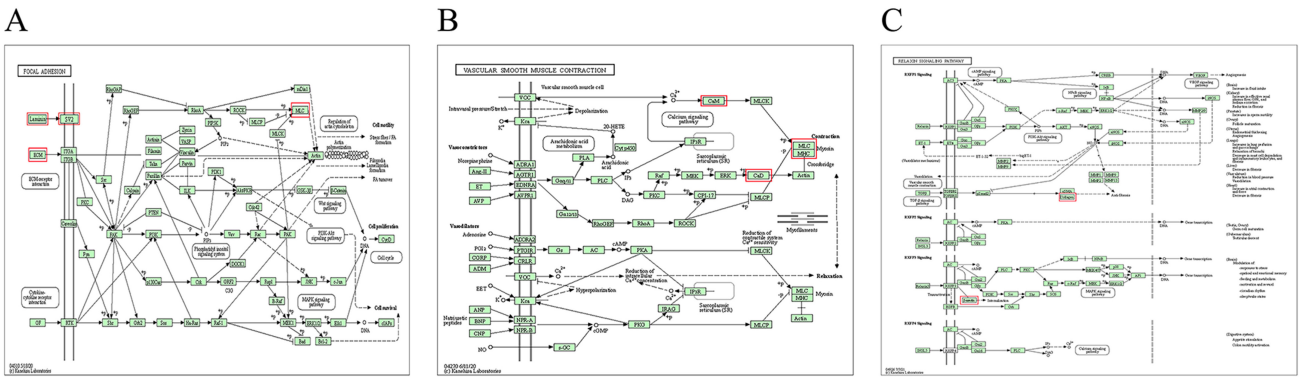

Fig. 7. KEGG signaling pathway diagram. The red boxes marked are the DEPs screened in this study. (A) is the relationship between ECM-receptor interaction, Focal adhesion and PI3K-Akt signaling pathway, (B) is the Vascular smooth muscle contraction pathway in which DEPs are involved, (C) is the relaxin signaling pathway in which DEPs are involved. Relaxin signaling pathway.

full range of biological effects on cellular activities through signal transduction pathways in vivo. It has been shown that in bladder smooth muscle, alterations in collagen fibers, elastic fibers, and adhesion proteins in the ECM seriously affect the function of bladder smooth muscle cells. We found that in cluster 1 Lama2, Lama4, Fn1, Fbn1, Lamb1, and Col3a1 are all ECM components (Fig. 6), and by analyzing the KEGG pathway of DEPs in cluster 1, we found that these DEPs mainly focus on ECM-receptor interaction, Focal adhesion, PI3K-Akt signaling pathway, relaxin signaling pathway and etc (Fig. 6). Previous studies have also found significant alterations in ECM components in bladder smooth muscle bundles after spinal cord injury, which remains consistent with our study. In normal bladder tissue, the contractility of smooth muscle cells is closely related to ECM, which may be related to the fact that ECM connects to the smooth muscle cell intracellular actin filaments through the corresponding receptors on the smooth muscle cell membrane, converting extracellular mechanical signals into chemical signals that ultimately affect the contractile properties of smooth muscle cells.

ECM has been found to activate focal adhesion kinase (FAK) *in situ* after binding to the integrin receptor on the cell membrane; FAK further binds and activates many signal proteins to regulate physiological activities, such as actin polymerization and cell migration, proliferation, and

apoptosis [17]. Previous studies have revealed that, in the gastric fundus smooth muscle, the phosphorylation of FAK can activate the calcium-sensitive signaling pathway and promote the contraction of the gastric fundus smooth muscle cells [18]; furthermore, in physiologically stretched smooth muscle in the bladder, the activation of FAK can enhance the contraction and proliferation of the smooth muscle cells [19]. Phosphorylated FAK can further activate the PI3K/Akt signaling pathway, which is related to biological processes such as cell proliferation, differentiation, protein synthesis, and actin polymerization [20]. Activated PI3K generates a second messenger, phosphatidylinositol-3,4,5-triphosphate (PIP3), on the cell membrane, which further activates p21-activated protein kinases (PAKs). PAK can inhibit the phosphorylation of myosin light chain kinase (MLCK) stimulated by acetylcholine to inhibit the contraction of smooth muscle cells [21]. Yiming Wang *et al.* [22] found that PAK regulates contraction mediated by α1-adrenoceptors in order to regulate the contraction of smooth muscle cells through adrenergic nerve fibers. In addition, the PIP3 complex can transport synaptic vesicles containing PIP3 from the cell body to axon terminals, and its directional transport function contributes to the local enhancement of the signal intensity of nerve terminals [23].

Synaptic vesicle glycoprotein 2A (Sv2A) in DEPs is involved in the signaling pathway of ECM-receptor interaction (Fig. 7A). Sv2A is a glycoprotein, specifically expressed in synaptic vesicles, that can regulate the release of neurotransmitters dependent on action potential. Recently, a study has reported that Sv2A has many potential functions, including vesicle transport, stabilizing the vesicle load of neurotransmitters, and regulating calcium sensitivity [24]. A previous study found that Sv2A-deficient mice had persistent seizures; levetiracetam, an anti-epileptic drug that targets Sv2A, has been widely used in clinical practice [25]. Another previous study identified that Sv2A overexpression can reduce the release of neurotransmitters [26]. This indicates that the abnormal increase or decrease of Sv2A expression may affect the release of neurotransmitters in synapses. Sv2A is not only expressed in the central nervous system but also controls the release of neurotransmitters by regulating the size of the easy-release pool in peripheral sympathetic synapses [27]. However, the bladder sphincter is mainly innervated by sympathetic nerves. In the present study, the expression of Sv2A in the bladder sphincters in the model group was significantly lower than in the blank group, which may be one of the reasons for the involuntary contraction of the bladder sphincter after T10 spinal cord injury.

The results of the present study found that the vascular smooth muscle contraction signaling pathway was significantly enriched, and we identified Calm2, Cald1 as the main DEPs involved in this signaling pathway (Fig. 6). In the study results, Calm2, a gene encoding calmodulin (CaM), and Cald1, a gene encoding calmodulin binding protein (CaD), were significantly elevated in the bladder sphincter of the model group. The change in Ca^{2+} concentration in the cytoplasm was the main factor affecting the contraction of the vascular smooth muscle cells [28]. The bladder sphincter is a smooth muscle, and its contraction depends on the concentration of Ca^{2+} in cytoplasm. Increased Ca^{2+} concentration activates the Ca^{2+}/calmodulin (CaM)/MLCK pathway and stimulates myosin light chain (MLC20) phosphorylation, resulting in myosin–myosin interaction, which leads to smooth muscle bundle contraction (see Fig. 7B). Therefore, the high expression of CaM can enhance the contractility of the smooth muscle bundle [29]. The CALM2 gene, which encodes calmodulin, and the CALD1 gene, which encodes calmodulin binding protein (CaD) in DEPs, participate in this signaling pathway and, in the present study, increased significantly in the bladder sphincters of the model group.

The abnormal expression of the CALM2 gene leads to the abnormal opening of the voltage-gated Ca^{2+} channel, sarcoplasmic reticulum Ca^{2+} release channel, and lanidine receptor subtype 2 plasma channel. CALM2 has also been classified as a gene that affects calcium treatment [30]. The CaD encoded by the CALD1 gene is a component of microfilaments in smooth muscle cells, and it can bind with actin, tropomyosin, calmodulin, and myosin to regulate the contraction of smooth muscle cells and the formation of a cytoskeleton [31]. In addition, Ca^{2+} plays a role in the contraction of smooth muscle cells and is a key ionic signal regulating the release of neurotransmitters through presynaptic membrane exocytosis. CaM and CaD together transmit the change in concentration of Ca^{2+} in cells to regulate the transport and exocytosis process of synaptic vesicles [32]. A recent study found that CaD affected the contraction of the bladder smooth muscle by acting as a molecular brake and maintaining the integrity of the contraction mechanism [33]; furthermore, in pathological bladder smooth muscle, the expression of contractile proteins (such as CaD) has been found to increase significantly [34]. Therefore, CaM and CaD may be one of the pathological mechanisms of non-inhibitory contraction of the bladder sphincter after SSCI.

In the relaxin signaling pathway, G-protein coupled receptor (GPCR) and relaxin family peptide receptor 1 (RXFP1) play an important role in promoting vasodilation and antifibrosis, activating nitrogenous nerve fibers and protecting the heart [35,36]. Edward *et al.* [37] found that RXFP1 was expressed in the smooth muscle cell layer of the human bladder triangle (where the bladder sphincter is located) and fornix, and expression of transforming growth factor β1 could be affected when the human bladder smooth muscle is stimulated with relaxin *in vitro*. Another study stated that relaxin-related receptors have become a drug target for the treatment of lower urinary tract fibrosis [38]. In addition to its antifibrotic effect, relaxin also produces a second messenger, nitric oxide (NO), to acti-

vate the NO/cyclic guanosine monophosphate/protein kinase G signaling pathway, thereby inhibiting the contraction of smooth muscle [39] (see Fig. 7C).

Arrestin β2 was first found in photoreceptors on the bovine retina. It participates in the signal transduction function of GPCR by mediating receptor desensitization and re-sensitization, competitively inhibiting the binding phosphorylated GPCR receptors to ligands. It also transports the corresponding receptor into the cell body after binding to the GPCR receptors, thus preventing the binding of the receptors to ligands [40]. A previous study revealed that GPCR is also involved in the activities of sympathetic and parasympathetic nerves: it binds to dopamine D1 receptors, muscarinic M2 receptors, α-adrenergic receptors, and β-adrenergic receptors, thus participating in more physiological processes regulated by the autonomic nervous system [41]. Another study found that the significant expression of arrestin β2 increases the internalization of α-adrenergic receptors on the cell membrane, preventing the binding of neurotransmitters to their corresponding receptors [42]. There are many α-adrenergic receptors on the cell membrane of the bladder sphincter; in sympathetic nerves the neurotransmitters released by α-adrenergic fibers can control the contraction of the bladder sphincter by binding α-adrenergic receptors to the cell membrane [43]. In the present study, the arrestin β2 in the bladder sphincters of the model group decreased significantly, which hindered the internalization of the α-adrenergic receptors. This may be one of the pathological mechanisms of non-inhibitory contraction of the bladder sphincter after SSCI.

5. Conclusions

It is of great significance to explore the pathological mechanism of non-inhibitory contraction of the bladder sphincter caused by spinal cord injury above the T10 segment from the perspective of ECM-receptor interaction, the focal adhesion-activated PI3K-Akt signaling pathway, the smooth muscle contraction signaling pathway, and the cell-relaxation signaling pathway. Sv2A, which is involved in the release of neurotransmitters from synaptic vesicles, arrestin β2, an inhibitory protein involved in the internalization of α-adrenergic receptors and GPCR receptors, and CaM and CaD, which are involved in the calcium-sensitive signaling pathway, may be potential targets for developing new ways to treat bladder sphincter overactivity caused by spinal cord injury.

It has been found that in patients with incomplete suprasacral spinal cord injuries (such as ASIA B, C spinal cord injuries) there is still a dysfunction of the detrusor-vesical sphincter synergy, and overactivity of the bladder sphincter may occur. For these conditions, clinical management can include inhibition of excessive bladder sphincter contraction as an important therapeutic idea. Therefore, incomplete spinal cord injury with overactive bladder sphincter can also consider the above-mentioned targets for intervention.

In this study, we screened for DEPs in the bladder sphincter after T10 spinal segment injury by TMT quantitative proteomics, however, we have not yet validated those DEPs that potentially modulate bladder sphincter contraction. We will continue to validate the screened DEPs to further explore these potential therapeutic targets and pathways for bladder sphincter overactivity.

Data availability

The data have been uploaded to ProteomeXchange with identifier PXD034595 (http://proteomecentral.proteomexchange.org/cgi/GetDataset?ID=PXD034595).

Author Contributions

Study design—KA, LZ. Project administration—KA, MX. Experiment implementation—QRQ, QL, XW. Data analysis—LYT, YYL, FQ. Paper writing—QRQ, LYT, KA. Paper review & editing—HZ. Experimental support—KA, LZ. All authors approved the final version of the manuscript.

Ethics Approval and Consent to Participate

Experimental animal ethics committee of Hunan University of Chinese Medcine. Ethical approval number: LL2019092303.

Acknowledgment

Not applicable.

Funding

General program of National Natural Science Foundation of China (81874510); University Student Innovation and Entrepreneurship Training Program Project of Hunan Province (S202110541019).

Conflict of Interest

The authors declare no conflict of interest.

References

[1] Zhang Q, Zhao FF, Liu TP, Wang CK, He XW. Research Progress of Acupuncture in the Treatment of Neurogenic Bladder after Spinal Cord Injury in Recent Ten Years. Jiang Xi Jouranl of Traditional Chinese Medicine. 2021; 52: 74–77.

[2] Xiong ZS, Xu ZY. Urodynamic study and classification of the bladder after spinal cord injury. Modern Rehabilitation. 2000; 805–807.

[3] Amarenco G, Sheikh Ismaël S, Chesnel C, Charlanes A, Le Breton F. Diagnosis and clinical evaluation of neurogenic bladder. European Journal of Physical and Rehabilitation Medicine. 2017; 53: 975–980.

[4] Mcbride AW. Pathphysio1gy of stress urinary incontinence. Journal of Pelvic Medicine and Surgery. 2004; 10: 1–7.

[5] Ke QS, Kuo HC. Transurethral incision of the bladder neck to treat bladder neck dysfunction and voiding dysfunction in pa-

tients with high-level spinal cord injuries. Neurourology and Urodynamics. 2010; 29: 748–752.
[6] Krongrad A, Sotolongo JR Jr. Bladder neck dysynergia in spinal cord injury. American Journal of Physical Medicine & Rehabilitation. 1996; 75: 204–207.
[7] Wyndaele JJ, Birch B, Borau A, Burks F, Castro-Diaz D, Chartier-Kastler E, *et al*. Surgical management of the neurogenic bladder after spinal cord injury. World Journal of Urology. 2018; 36: 1569–1576.
[8] Romo PGB, Smith CP, Cox A, Averbeck MA, Dowling C, Beckford C, *et al*. Non-surgical urologic management of neurogenic bladder after spinal cord injury. World Journal of Urology. 2018; 36: 1555–1568.
[9] Chen C, Hou J, Tanner JJ, Cheng J. Bioinformatics Methods for Mass Spectrometry-Based Proteomics Data Analysis. International Journal of Molecular Sciences. 2020; 21: 2873.
[10] Wang Z, Kavdia K, Dey KK, Pagala VR, Kodali K, Liu D, *et al*. High-throughput and Deep-proteome Profiling by 16-plex Tandem Mass Tag Labeling Coupled with Two-dimensional Chromatography and Mass Spectrometry. Journal of Visualized Experiments. 2020; 10.3791/61684.
[11] Shaker H, Mourad MS, Elbialy MH, Elhilali M. Urinary bladder hyperreflexia: a rat animal model. Neurourology and Urodynamics. 2003; 22: 693–698.
[12] Scheff SW, Saucier DA, Cain ME. A Statistical Method for Analyzing Rating Scale Data: the BBB Locomotor Score. Journal of Neurotrauma. 2002; 19: 1251–1260.
[13] Xie C, Mao X, Huang J, Ding Y, Wu J, Dong S, *et al*. KOBAS 2.0: a web server for annotation and identification of enriched pathways and diseases. Nucleic Acids Research. 2011; 39: W316–W322.
[14] Bindea G, Mlecnik B, Hackl H, Charoentong P, Tosolini M, Kirilovsky A, *et al*. ClueGO: a Cytoscape plug-in to decipher functionally grouped gene ontology and pathway annotation networks. Bioinformatics. 2009; 25: 1091–1093.
[15] Su G, Morris JH, Demchak B, Bader GD. Biological Network Exploration with Cytoscape 3. Current Protocols in Bioinformatics. 2014; 47: 8.13.1–8.13.24.
[16] Zhu Y, Huang J, Cheng J, Zhang WY, Yu J, Zhu LT. Effects of electro-acupuncture on myoelectric activity of detrusor and external urethra sphincter of complete T10 level spinal cord transection rats. Chinese Journal of Rehabilitation Medicine. 2013; 28: 124–128.
[17] Sweeney HL, Hammers DW. Muscle Contraction. Cold Spring Harbor Perspectives in Biology. 2018; 10: a023200.
[18] Xie Y, Han KH, Grainger N, Li W, Corrigan RD, Perrino BA. A role for focal adhesion kinase in facilitating the contractile responses of murine gastric fundus smooth muscles. The Journal of Physiology. 2018; 596: 2131–2146.
[19] Luo D, Wazir R, Tian Y, Yue X, Wei T, Wang K. Integrin αv Mediates Contractility whereas Integrin α4 Regulates Proliferation of Human Bladder Smooth Muscle Cells via FAK Pathway under Physiological Stretch. Journal of Urology. 2013; 190: 1421–1429.
[20] Xie P, Kondeti VK, Lin S, Haruna Y, Raparia K, Kanwar YS. Withdrawal: Role of extracellular matrix renal tubulointerstitial nephritis antigen (TINag) in cell survival utilizing integrin αvβ3/focal adhesion kinase (FAK)/phosphatidylinositol 3-kinase (PI3K)/protein kinase B-serine/threonine kinase (AKT) signaling pathway. Journal of Biological Chemistry. 2019; 294: 10379.
[21] [21] Murthy KS, Zhou H, Grider JR, Brautigan DL, Eto M, Makhlouf GM. Differential signalling by muscarinic receptors in smooth muscle: m2-mediated inactivation of myosin light chain kinase via Gi3, Cdc42/Rac1 and p21-activated kinase 1 pathway, and m3-mediated MLC20 (20 kDa regulatory light chain of myosin II) phosphorylation via Rho-associated kinase/myosin phosphatase targeting subunit 1 and protein kinase C/CPI-17 pathway. Biochemical Journal. 2003; 374: 145–155.
[22] Wang Y, Gratzke C, Tamalunas A, Wiemer N, Ciotkowska A, Rutz B, *et al*. P21-Activated Kinase Inhibitors FRAX486 and IPA3: Inhibition of Prostate Stromal Cell Growth and Effects on Smooth Muscle Contraction in the Human Prostate. PLoS ONE. 2016; 11: e0153312.
[23] Horiguchi K, Hanada T, Fukui Y, Chishti AH. Transport of PIP3 by GAKIN, a kinesin-3 family protein, regulates neuronal cell polarity. Journal of Cell Biology. 2006; 174: 425–436.
[24] Stout KA, Dunn AR, Hoffman C, Miller GW. The Synaptic Vesicle Glycoprotein 2: Structure, Function, and Disease Relevance. ACS Chemical Neuroscience. 2019; 10: 3927–3938.
[25] Ohno Y, Tokudome K. Therapeutic Role of Synaptic Vesicle Glycoprotein 2a (SV2a) in Modulating Epileptogenesis. CNS and Neurological Disorders - Drug Targets. 2017; 16: 463–471.
[26] Nowack A, Malarkey EB, Yao J, Bleckert A, Hill J, Bajjalieh SM. Levetiracetam reverses synaptic deficits produced by overexpression of SV2A. PLoS ONE. 2011; 6: e29560.
[27] Vogl C, Tanifuji S, Danis B, Daniels V, Foerch P, Wolff C, *et al*. Synaptic vesicle glycoprotein 2a modulates vesicular release and calcium channel function at peripheral sympathetic synapses. European Journal of Neuroscience. 2015; 41: 398–409.
[28] Touyz RM, Alves-Lopes R, Rios FJ, Camargo LL, Anagnostopoulou A, Arner A, *et al*. Vascular smooth muscle contraction in hypertension. Cardiovascular Research. 2018; 114: 529–539.
[29] Mizuno Y, Isotani E, Huang J, Ding H, Stull JT, Kamm KE. Myosin light chain kinase activation and calcium sensitization in smooth muscle in vivo. American Journal of Physiology-Cell Physiology. 2008; 295: C358–C364.
[30] Wleklinski MJ, Kannankeril PJ, Knollmann BC. Molecular and tissue mechanisms of catecholaminergic polymorphic ventricular tachycardia. The Journal of Physiology. 2020; 598: 2817–2834.
[31] Lin JJ, Li Y, Eppinga RD, Wang Q, Jin JP. Chapter 1 Roles of Caldesmon in Cell Motility and Actin Cytoskeleton Remodeling. International Review of Cell and Molecular Biology. 2009; 274: 1–68.
[32] Liang C, Zhang G, Zhang L, Chen S, Wang J, Zhang T, *et al*. Calmodulin Bidirectionally Regulates Evoked and Spontaneous Neurotransmitter Release at Retinal Ribbon Synapses. Eneuro. 2021; 8: ENEURO.0257–ENEU20.2020.
[33] Pütz S, Barthel LS, Frohn M, Metzler D, Barham M, Pryymachuk G, *et al*. Caldesmon ablation in mice causes umbilical herniation and alters contractility of fetal urinary bladder smooth muscle. Journal of General Physiology. 2021; 153: e202012776.
[34] Vaes RDW, van den Berk L, Boonen B, van Dijk DPJ, Olde Damink SWM, Rensen SS. A novel human cell culture model to study visceral smooth muscle phenotypic modulation in health and disease. American Journal of Physiology-Cell Physiology. 2018; 315: C598–C607.
[35] Valkovic AL, Bathgate RA, Samuel CS, Kocan M. Understanding relaxin signalling at the cellular level. Molecular and Cellular Endocrinology. 2019; 487: 24–33.
[36] Martin B, Romero G, Salama G. Cardioprotective actions of relaxin. Molecular and Cellular Endocrinology. 2019; 487: 45–53.
[37] Diaz EC, Briggs M, Wen Y, Zhuang G, Wallace SL, Dobberfuhl AD, *et al*. Characterizing relaxin receptor expression and exploring relaxin's effect on tissue remodeling/fibrosis in the human bladder. BMC Urology. 2020; 20: 44.
[38] Andersson K, Fry C, Panicker J, Rademakers K. Which molecular targets do we need to focus on to improve lower urinary tract dysfunction? ICI-RS 2017. Neurourology and Urodynamics. 2018; 37: S117–S126.
[39] Lian X, Beer-Hammer S, König GM, Kostenis E, Nürnberg B,

Gollasch M. RXFP1 Receptor Activation by Relaxin-2 Induces Vascular Relaxation in Mice via a Gα i2-Protein/PI3Kß/γ/Nitric Oxide-Coupled Pathway. Frontiers in Physiology. 2018; 9: 1234.

[40] Matthees ESF, Haider RS, Hoffmann C. B-arrestin–based biosensors: Tools to explore structural determinants of metabolic functions? Current Opinion in Endocrine and Metabolic Research. 2021; 16: 66–74.

[41] Gao H, Sun Y, Wu Y, Luan B, Wang Y, Qu B, *et al*. Identification of beta-arrestin2 as a G protein-coupled receptor-stimulated regulator of NF-kappaB pathways. Molecular Cell. 2004; 14: 303–317.

[42] Stanasila L, Abuin L, Dey J, Cotecchia S. Different internalization properties of the alpha1a- and alpha1b-adrenergic receptor subtypes: the potential role of receptor interaction with beta-arrestins and AP50. Molecular Pharmacology. 2008; 74: 562–573.

[43] Akinaga J, García-Sáinz JA, S Pupo A. Updates in the function and regulation of α 1 -adrenoceptors. British Journal of Pharmacology. 2019; 176: 2343–2357.